

Thermal Cycle Fatigue Life of Low-Temperature Solders

Michael Osterman, Ph.D., Aaron Mendelsohn
CALCE/University of Maryland
MD, USA
osterman@umd.edu; amendell@umd.edu

ABSTRACT

Solder interconnects are required to provide low resistance connections between terminals of packaged devices and printed boards over the expected life. Thermal cycling fatigue is one of the main reliability concerns for solder. For the introduction of low temperature solders with reflow peak temperatures below 200°C, their thermal cycle fatigue life must be characterized. This paper presents a multiple component type test and time to failure data for solder interconnects formed with low temperature solders for BGAs, QFNs, and SMR component types.

Key words: low-temperature solder, thermal cycling

INTRODUCTION

With the trend towards electronics with thinner profiles, warpage of components during the printed board assembly processes has become a concern. To address this issue, manufacturers are examining and adopting low temperature solders. Research has focus on eutectic and near eutectic tin-bismuth (SnBi) solders which can allow for reflow assembly below peak temperatures of 200 °C [1]. Eutectic SnBi melts at 138°C, while the industry standard solder, SAC305, has a melting temperature around 217°C. For reflow assembly, the peak temperatures in the assembly can 30°C higher than the solder melt temperature. The reduction in peak reflow temperature by as much as 80°C greatly reduces the risk of component warpage and minimizes the risk for solder reflow assembly issues. While the use of low temperature solder reduces risk of reflow assembly issues, the ability of the solder interconnects to meet life cycle loading requirements must still be assessed.

While studies on temperature cycle performance of low temperature solders have been conducted, further work is needed to understand how fatigue failure occurs in low temperature SnBi based soldered. In addition, variation of low temperature solder with additions of antimony and silver are being examined to improve solder durability. This paper presents a study of 3 different SnBi based low temperature solders with two low temperature solders having antimony and silver additions. For comparison, SAC305 is included. The differences in thermal cycle fatigue life based on solder compositions are examined. Different component type (BGA, MLF, Resistor) is included to isolate the influence of the solder composition from that of the package geometry. The BGA packages have SAC305 solder spheres resulting in hybrid solder interconnects. This variation in packages and

mixing in the hybrid solder interconnects is expected to provide insight in the field reliability.

EXPERIMENT

The printed board assembly vehicles are designed to mount 24 components, of which there are 5 different component types, in groups of 4 identical components each. These components are CTBGA228, CVBGA360, CABGA192, 68LD/MLF, and 1206 resistors. The components are test parts designed to form a low electrical resistance path when solder attached to a printed board to form a daisy chain resistance path through the component terminals.

The four-layer printed boards are fabricated with FR4 and are 9 x 4.5 x 0.0063 inches. The solder pads are finished with organic solder preservative (OSP). The board copper patterns are designed to allow independent electrical resistance monitoring through all solder interconnects for each component solder to the board. These test boards are designed with connections between edge pads and the footprint of each component. When the components are soldered to the printed board, the connections create single resistance paths for each component that include all component solder interconnects.

Based on prior studies, solder paste to solder sphere volume in creating hybrid interconnects with low temperature solder and SAC305 BGAs has been reported to be between 50 to 70% [2]. For the surface mount 1206 resistors, each printed board provides four positions with regular 1206 pads and four positions with pads designed half the regular 1206 pad width. Table 1 provides the specifications of each component and Figure 1 presents a picture of an assembled test board.

Table 1: Component Details

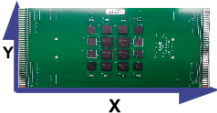


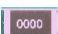


Components	Count
CVBGA360, SAC305 Ball Dia. 0.25 mm, Pitch 0.4 mm	4
CTBGA228, SAC305 Ball Dia. 0.3 mm, Pitch 0.5 mm	4
CABGA192, SAC305 Ball Dia. 0.46 mm, Pitch 0.8 mm	4
MLF68, Pitch 0.5 mm	4
1206 Resistor (50% Pad Width)	4
1206 Resistor	4



Figure 1: Printed Board Assembly Test Sample

For analysis purposes, the coefficient of temperature expansion (CTE) measurements of the components and board involved were determined using either a thermo-mechanical analyzer or micro-Moiré interferometry. These values are presented in Table 2.

Table 2: Elemental analysis of LTS 1-5, using XRF

Thermo-Mechanical Analysis		Moiré Interferometry									
<div>Board</div> <div></div> <table><thead><tr><th>Direction</th><th>CTE < T_g = 120°C</th></tr></thead><tbody><tr><td>X</td><td>12.1 ppm/°C</td></tr><tr><td>Y</td><td>13.8 ppm/°C</td></tr><tr><td>Z</td><td>48.4 ppm/°C</td></tr></tbody></table>		Direction	CTE < T _g = 120°C	X	12.1 ppm/°C	Y	13.8 ppm/°C	Z	48.4 ppm/°C	<div>CABGA192</div> <div></div> <div>CTE</div> <div>7.6 (ppm/°C)</div>	<div>CVBGA360</div> <div></div> <div>CTE</div> <div>12.1 (ppm/°C)</div>
Direction	CTE < T _g = 120°C										
X	12.1 ppm/°C										
Y	13.8 ppm/°C										
Z	48.4 ppm/°C										
<div>SM1206</div> <div></div> <div>CTE</div> <div>4.3 (ppm/°C)</div>		<div>MLF68</div> <div></div> <div>CTE</div> <div>16.7 (ppm/°C)</div>	<div>CTBGA228</div> <div></div> <div>CTE</div> <div>10.8 (ppm/°C)</div>								

Four solders were used for this study: SAC305 for control and three different Sn-Bi based low-temperature solders. These solders with elemental percent weight identified by XRF are presented in Table 3.

Table 3: Solders Under Test

<u>Solder Identifiers</u>	<u>XRF Measurement</u>
<u>SAC</u>	<u>Sn3.0Ag0.5Cu</u>
<u>LTS1</u>	<u>Sn62.4Bi0.03Cu</u>
<u>LTS2</u>	<u>Sn64.4Bi0.81Sb</u>
<u>LTS3</u>	<u>Sn54.9Bi0.4Ag0.3Sb</u>

The elemental weight measurements were taken on solder connector pads from the test printed board assemblies. Measurements were taken 10 times and average values are presented.

The reflow parameters for the SAC305 assemblies are presented in Table 4 and the parameters for the low temperature solder are presented in Table 5.

Table 4: Reflow parameters for SAC solders

Reflow Parameter	Value
Time between 150 and 200C	75 sec
Time above 220°C	65sec
Ramp up after 220°C	0.43 °C/sec
Peak	241 °C
Cooldown	-1.36 °C/sec

Table 5: Reflow parameters for Low Temperature solders

Reflow Parameter	Value
Time between 130 and 150C	80 sec
Time above 150°C	86 sec
Ramp up after 150°C	0.715 °C/sec
Peak	186 °C
Cooldown	-0.985 °C/sec

Experiments

The bismuth distribution in the BGA parts was characterized through inspection of mechanical cross-sections under a scanning electron microscope (SEM).

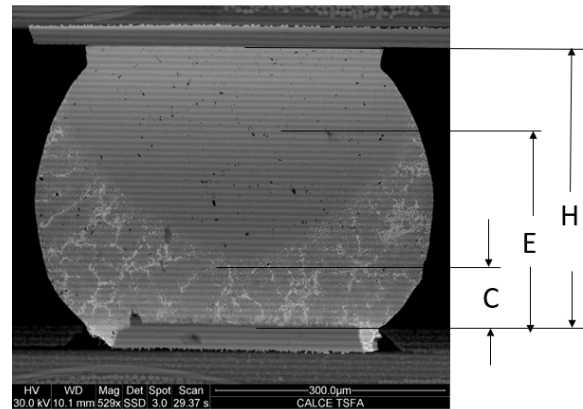


Figure 2: Measures of Bismuth Distribution in BGAs

Measurements included the height of the solder interconnect from pad to pad, H, the distance from the printed board pad to the end of the bismuth at the outer edge of the BGA sphere, E, and the height of the bismuth above the printed board pad at the center of the BGA, C, for each of the three BGA parts under test. Figure 2 depicts the measurements that were made.

Solder interconnect thermal cycle fatigue life was measured by placing test specimens in a thermal cycling chamber programmed to cycle between a temperature of -50 °C to 100 °C with 15-minute dwell periods at the two temperature extremes. The rate of temperature change was approximately 7 °C/ min. Thermal cycle induced solder interconnect fatigue

life is known to depend on the temperature range, the mean cycle temperature, the dwell times, and to a lesser degree on ramp rate.

For the test, two test specimens for each solder were placed in the thermal cycle chamber. The resistance path for each component on each test specimen were monitored using an Agilent 34980 datalogger. In addition to the resistance of each component resistance path, 10 thermocouples were also placed in the chamber and connected to the datalogger. The datalogger record temperature can resistance values every minute. Failure was identified by resistance increase of 1000 ohms with resistance greater than 20 ohms above initial maximum recorded value. The test was terminated after 7056 cycles.

After the test was terminated, the test boards were inspected for visible signs of failure. In addition, components identified to have failed were electrically tested to verify datalogger identification. After confirmation, select soldered component board samples were exercised from the board for cross-sectional analysis. Unfortunately, the MLF68 components, which failed early in the test, either fell off in the test chamber during the test or were dislodged when removing them from the chamber. As a result, microsections of the MLF68 components are unavailable.

EXPERIMENTAL RESULTS

The sectional analysis of each BGA type is presented in Tables 3 through 5.

Table 5: Bismuth Distribution for CABGA192 components

	H μm		E μm		C μm	
	ave	stdev	ave	stdev	ave	stdev
SAC305	296	5				
LTS1	353	12	237	33	132	12
LTS2	368	5	266	13	82	16
LTS3	399	10	249	10	73	13

Table 6: Bismuth Distribution for CTBGA228 components

	H μm		E μm		C μm	
	ave	stdev	ave	stdev	ave	stdev
SAC305	190	5				
LTS1	179	3	80	7	58	5
LTS2	239	5	164	10	90	4
LTS3	232	5	126	19	82	11

Table 7: Bismuth Distribution for CVBGA360 components

	H μm		E μm		C μm	
	ave	stdev	ave	stdev	ave	stdev
SAC305	204	2				
LTS1	196	4	63	6	21	4
LTS2	248	3	123	9	80	12
LTS3	224	2	105	15	65	8

Since the solder interconnect height places a role in its thermal cycle fatigue life [3], it is interesting to note that the solder interconnect height for the exceeds the low temperatures solders for the CABGA192 parts. This is likely due to the overprinting that was applied to ensure as greater than 50% paste to solder sphere ratio use for the BGA parts. For the various LTS solders, LTS1 solder interconnect heights were the shortest for all BGA components. The LTS1 solder interconnect height was also less than SAC305 for the CTBGA228 and the CVBGA360 components. The bismuth diffusion reflected in edge and center height followed the interconnect heights for the LTS solder for the CTBGA and CVBGA360 components. However, this was not the case for the CABGA192 components. More on these observations will be discussed as part the cross-section analysis of failures interconnects from the thermal cycle tests.

As mention earlier, the test was stopped after 7056 thermal cycles. In the following paragraphs the test results along with representative cross-sections of fully or partially solder fatigue cracks in solder interconnects will be present. Test data include a break down by solders number of failure recorded, cycles to first failure and cycles to last recorded failure. In addition, a 2-parameter Weibull distribution analysis results and probability of failure versus thermal cycle count plots are presented along with sectional analysis.

Table 8 provides the thermal cycle test summary for the MLF68 components. In figure 8, the failure data for the MLF68 component is plotted. For the MLF68 component without center pad attachment, LTS 1-3 outperformed SAC305. Interestingly, the LTS3 with measured antimony and silver, outperformed LTS1 and LTS2.

Table 8: Failure Summary Table for MLF68

MLF68	#F	%F	First	Last
SAC	8/8	100	500	1971
LTS1	8/8	100	1315	1686
LTS2	8/8	100	1357	1735
LTS3	8/8	100	1597	1872

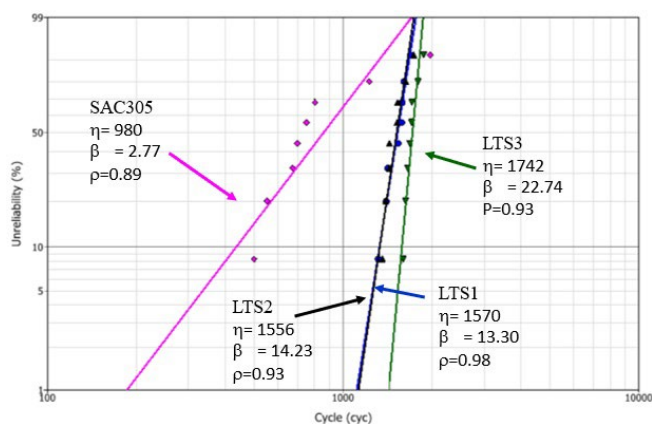


Figure 8: Weibull Plot for MLF68 Components

Table 9 provides a summary for the CTBGA228 components with all components failing prior to the termination of the test. In figure 9, the failure data for the CTBGA228 component is plotted. For the CTBGA228 component, the characteristic life followed the order to the numbers assigned to the solders and SAC305 presented with the lowest characteristic life. While the characteristic life values demonstrate a similar order that was observed with the MLF68 components, the early recorded failure overlap making the significance of the observation unclear. This result may be in part due to the small sample size. It may also be the nature of the mixed LTS and SAC305 solder interconnects. The solder interconnect height may also play a role.

Table 9: Failure Summary Table for CTBGA228

CTBGA288	#F	%F	First	Last
SAC	8/8	100	1761	2929
LTS1	8/8	100	1777	3615
LTS2	8/8	100	1647	3898
LTS3	8/8	100	2118	3821

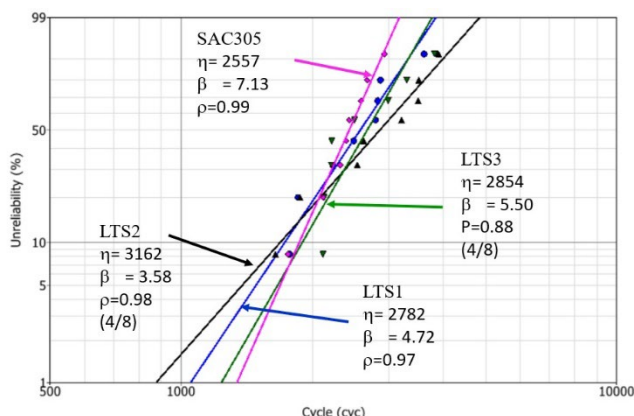


Figure 9: Weibull Plot for CTBGA228 Components

Sectional analysis of failed solder interconnects found failures at both the solder to board pad and the solder to component pad interfaces. Present analysis has not established the most likely side of fatigue crack formation.

Figure 10 depicts the failure of LTS2 mixed solder interconnect with failure occurring at the component to solder interface. In the image, the bismuth is distributed throughout the solder interconnect with enlarged bismuth regions at the solder to board interface. Figure 11 depicts the LTS3 mixed solder interconnect with the failure near the solder to board pad interface, however

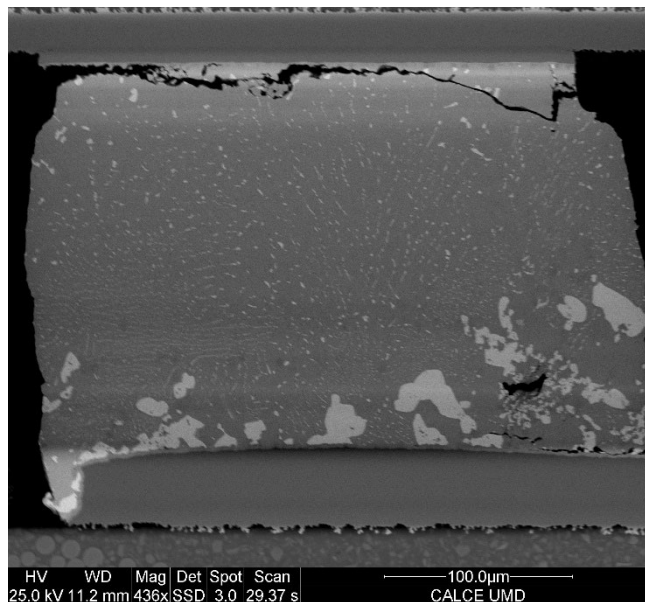


Figure 10: CTBGA228 LTS2 Solder Interconnect

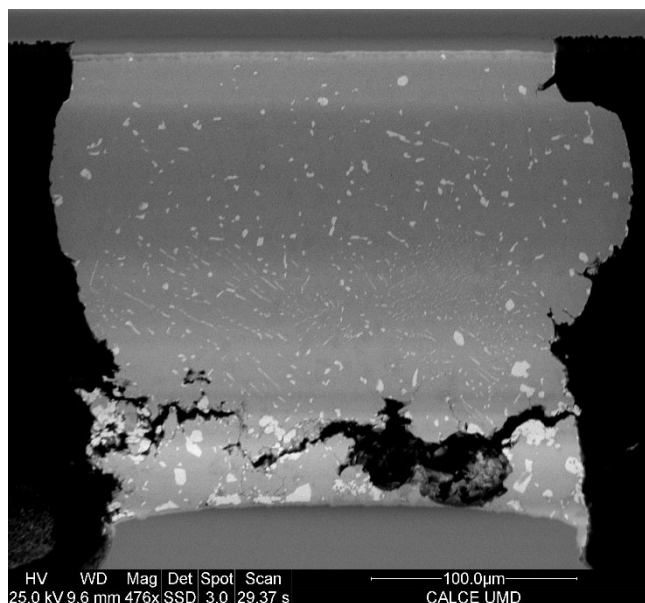


Figure 11: LTS3 CTBGA228 Interconnect

Table 10 provides a summary for the CVBGA360 components with all components failing prior to the termination of the test. In Figure 12, the failure data is presented using a 2 parameter Weibull analysis.

For the CVBGA360 components, the LTS alloys outperformed SAC305. However, LTS1 presented with initial failures prior to SAC305 and a characteristic life less

than half of the LTS2 and LTS3 soldered CVBGA360 components. It should be noted that the order of failure for the CVBGA360 components followed the pattern presented by the MLF68 components

Table 10: Failure Summary for CVBGA360

CVBGA360	#F	%F	First	Last
SAC	8/8	100	1841	3361
LTS1	8/8	100	1744	5506
LTS2	4/8	50	3376	6238
LTS3	4/8	50	3562	6357

Figure 13 presents a SEM image of a fatigue damaged solder interconnect from a CVBGA360 component assemblies with LTS1. At this writing, LTS CVBGA360 interconnects have not be found with fatigue cracks completely separating the component and board sides of the interconnect. It is likely that these cracks are present closer to the die region of the components. In review the current partially fatigue crack solder interconnects, the distribution of bismuth throughout the solder interconnect can be observed with the enlarged bismuth regions near the pad on the printed board.

Figure 14 presents a SEM image of a fatigue crack near the component pad in a SAC305 CVBGA360 that complete separates the component side from the board side.

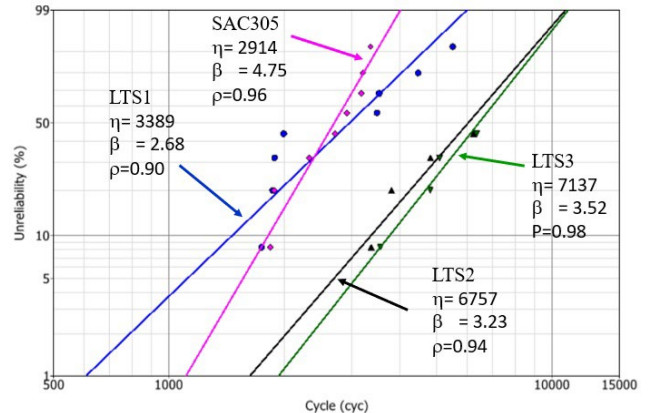


Figure 12: Weibull Plot for CVBGA360 Components

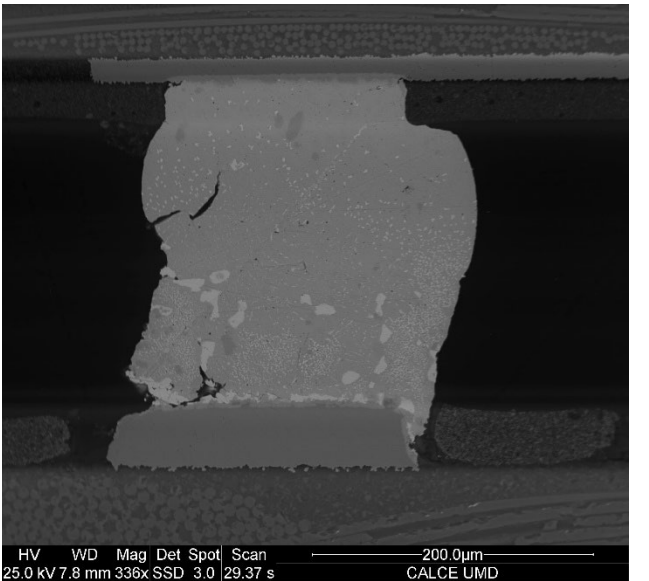


Figure 13: LTS1 CVBGA Solder Interconnect with Fatigue Damage

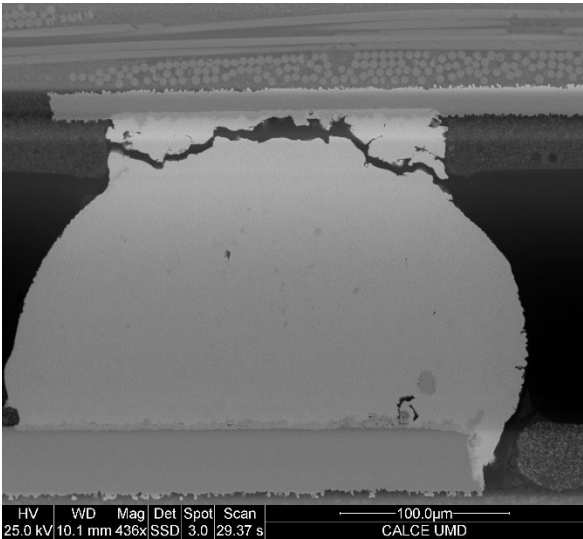


Figure 14: SAC305 CVBGA360 Solder Interconnect

Table 11 presents a summary of the failures for the CABGA192 components. In Figure 15, the failure data for the CABGA192 package is plotted. There was a novel lack of failure among the CABGA192 components attached with LTS1 and LTS2. LTS3 had very similar performance to SAC305 under thermal cycling.

Table 11: Failure Summary for CABGA192 Components

SM1206N	#F	%F	First	Last
SAC	8/8	100	4263	6762
LTS1	0/8	0		
LTS2	0/8	0		
LTS3	6/8	72	3562	6781

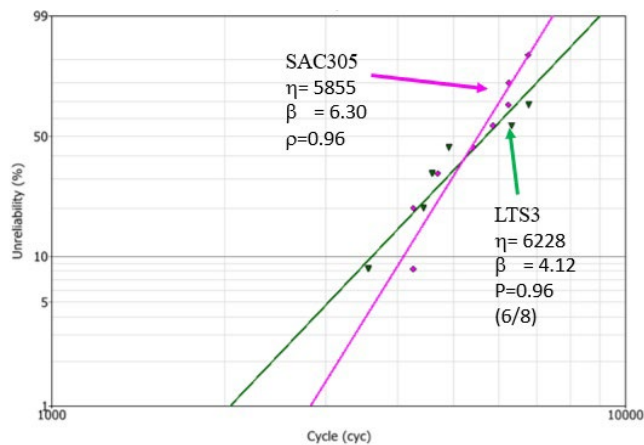


Figure 15: Weibull Plot for CABGA192 components

From the Weibull plot of the CABGA192, we observe a crossing of the probability of failure line between the SAC305 and mixed SAC305/LTS3 interconnects. Analysis of a SAC305/LTS3 thermal cycled interconnect depicts migration of bismuth into the SAC305 region as well and enlargement for bismuth regions near the printed board pad side of the solder interconnect.

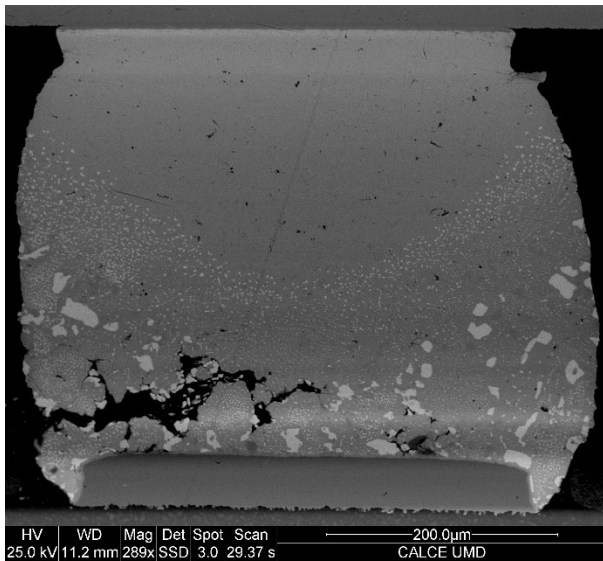


Figure 16: LTS3 CABGA192 Interconnect with a Partial Fatigue Crack

Table 12 provides a summary of the failures for the SMR1206 components attached to the narrow pad locations. In Figure 14, the failure data for the SMR1206 component is plotted. Few resistors failed in all solders, resulting in a smaller sample size of failure across the board. LTS2 had only 2 failures, while LTS1 had three failures. LTS3 had four failure and SAC305 had 5 failures.

Table 12: Failure Summary for SMR1206 Narrow Pad Components

SM1206N	#F	%F	First	Last
SAC	5/8	62.5	2830	4549
LTS1	3/8	37.5	5604	6261
LTS2	2/8	25	6254	6817
LTS3	4/8	50	4521	6245

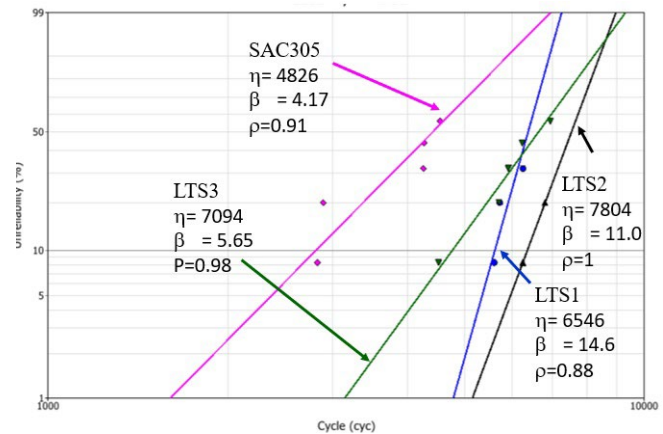


Figure 17: Weibull Plot for SMR1206 Interconnects with Narrow Pads

From the Weibull plot of the SMR1206 components attached to the narrow board pads, SAC305 remains the interconnect with the lowest characteristic life. For the low temperature solders, LTS1 presents with the lowest characteristic life. However, LTS3 is the first to failure among the LTS solder. Figure 18 presents a SEM image of a LTS3 SMR1206 interconnect. In examining the microstructure, enlarged bismuth regions are observed. This behavior was observed in all LTS interconnects.

SUMMARY

The results of this experiment reflect an increased lifetime under thermal cycling conditions for LTS 1-3, as compared to SAC305. This outcome highlights the advantages which hybrid SnBi interconnects have over SAC305 solder in particular. This increase in average lifetime indicates characteristics in enhanced SnBi solder which are more desirable to manufacturers than the current characteristics of SAC305. These characteristic differences may be used as rationale for prioritization of SnBi use over that of SAC305. More study should be performed into the other mechanical characteristics of enhanced SnBi solder to come to any definitive conclusions, including greater focus on the impact of dwell times on thermal stresses due to CTE. However, these results are still strong reason to consider usage of these solders in most applications.

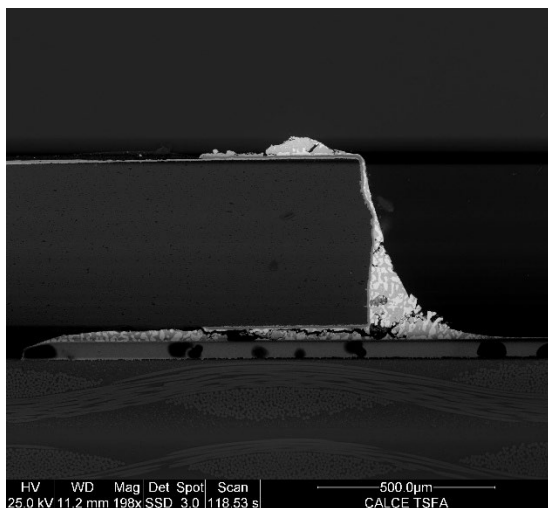


Figure 18: LTS1 SMR1206 Interconnect

The results of this experiment reflect an increased lifetime under thermal cycling conditions for the low temperature solders as compared to SAC305. This outcome highlights the advantages of low temperature solder for applications with thermal cycle challenges. Hybrid interconnects present a mixed result with some hybrid SAC305 and low temperature solder be nearly equivalent to SAC305 while other being superior. Enhancements with the addition of antimony and silver present appear to provide an improvement over simple tin-bismuth solder. This increase in average lifetime indicates characteristics in enhanced SnBi solder which are more desirable to manufacturers than the current characteristics of SAC305. These characteristic differences may be used as rationale for prioritization of enhanced SnBi use over that of SAC305. However, more study should be performed into the other mechanical characteristics of enhanced SnBi solder to come to any definitive conclusions, including greater focus on the impact of dwell times on thermal stresses due to CTE. However, these results are still strong reason to consider usage of these solders in most applications.

REFERENCES

- [1] A. Allen, H. Holder, E. Benedetto, B. Shi, K. Chn, D. Pipho, and V. Sakthi., Test Data Requirements for the Acceptance of Low Temperature Solder Alloys, SMTA International, Oct 2022, pp. 399-408
- [2] Akkara, F., Su, S., Ali, H., and Borgesen, P., "Effect of Cycling Amplitude Variations on SnAgCu Solder Joint Fatigue Life," IEEE Trans. Components, Packaging, and Manufacturing Technology, 2018, 8(11), pp. 1896–1904.
- [3] Elviz George, Michael Osterman and Michael Pecht , "An evaluation of dwell time and mean cyclic temperature parameters in the Engelmaier model," Microelectronics Reliability 55, Feb - March 2015, DOI:10.1016/S0026-2714(15)00039-6, pp 582-587.